


Provided by the author(s) and University College Dublin Library in accordance with publisher policies. Please cite the published version when available.

Title	Photo-catalytic degradation of an oil-water emulsion using the photo-Fenton treatment process : effects and statistical optimization
Author(s)	Tony, Maha A.; Purcell, Patrick J.; Zhao, Y.Q.; Tayeb, Aghareed M.; El-Sherbiny, M.F.
Publication date	2009-01
Publication information	Journal of Environmental Science and Health, Part A, 44 (2): 179-187
Publisher	Taylor & Francis
Link to online version	http://dx.doi.org/10.1080/10934520802539830
Item record/more information	http://hdl.handle.net/10197/3136
Publisher's statement	This is an electronic version of an article published in Journal of Environmental Science and Health, Part A: Toxic/Hazardous Substances & Environmental Engineering, 44 (2): 179-187, available online at: http://www.tandfonline.com/doi/abs/10.1080/10934520802539830
Publisher's version (DOI)	http://dx.doi.org/10.1080/10934520802539830

Downloaded 2018-10-22T15:49:45Z

The UCD community has made this article openly available. Please share how this access benefits you. Your story matters! (@ucd_oa) 

Some rights reserved. For more information, please see the item record link above.



1
2 **Photo-Catalytic Degradation of an Oil-Water Emulsion Using the Photo-Fenton**
3 **Treatment Process: Effects and Statistical Optimization**

4
5 MAHA A. TONY^{1,2}, P.J. PURCELL^{1*}, Y.Q. ZHAO¹, A.M. TAYEB³, M.F. EL-SHERBINY²
6

7 ¹ *Centre for Water Resources Research, School of Architecture, Landscape and Civil Engineering,*
8 *University College Dublin, Newstead, Belfield, Dublin 4, Ireland*

9 ² *Basic Engineering Science Department, Faculty of Engineering, Minoufiya University, Minoufiya,*
10 *Egypt*

11 ³ *Chemical Engineering Department, Faculty of Engineering, Minia University, Minia, Egypt*
12

13
14 **ABSTRACT**

15 The application of advanced oxidation processes (AOPs) to the treatment of an effluent
16 contaminated with hydrocarbon oils was investigated. The AOPs conducted were Fe²⁺/H₂O₂
17 (Fenton's reagent), Fe²⁺/H₂O₂/UV (Photo-Fenton's reagent) and UV-photolysis. These technologies
18 utilize the very strong oxidizing power of hydroxyl radicals to oxidize organic compounds to
19 harmless end products such as CO₂ and H₂O. A synthetic wastewater generated by emulsifying
20 diesel oil and water was used. This wastewater might simulate, for example, a waste resulting from
21 a hydrocarbon oil spill, onto which detergent was sprayed. The experiments utilising the Photo-
22 Fenton treatment method with an artificial UV source, coupled with Fenton's reagent, suggest that
23 the hydrocarbon oil is readily degradable, but that the emulsifying agent is much more resistant to
24 degradation. The results showed that the COD (chemical oxygen demand) removal rate was
25 affected by the Photo-Fenton parameters (Fe²⁺, H₂O₂ concentrations and the initial pH) of the
26 aqueous solution. In addition, the applicability of the treatment method to a 'real' wastewater
27 contaminated with hydrocarbon oil is demonstrated. The 'real' wastewater was sourced at a nearby
28

29 * Address correspondence to P.J. Purcell, Centre for Water Resources Research, School of
30 Architecture, Landscape and Civil Engineering, University College Dublin, Newstead, Belfield,
31 Dublin 4, Ireland; Phone: +353 1 7163216, fax: +353 1 7163297; E-mail address: pj.purcell@ucd.ie
32

33 car-wash facility located at a petroleum filling station and the experimental results demonstrate the
34 effectiveness of the treatment method in this case. A statistical analysis of the experimental data
35 using the Statistical Analysis System (SAS) and the response surface methodology (RSM) based on
36 the experimental design was applied to optimize the Photo-Fenton parameters (concentrations of
37 Fe^{2+} , H_2O_2 and initial pH) and to maximize the COD removal rate (more than 70%).

38
39 **Key Words:** Fenton, Photo-Fenton, diesel oil, wastewater, photo-catalysis, response surface
40 methodology

42 INTRODUCTION

43 As a result of human activities, there are many accidental discharges of hydrocarbon oil to the
44 natural environment during its processing, transportation and storage. For example, it is estimated
45 that, in US alone, at least 2 million litres of petroleum are spilled annually. ^[1] Oil-spills cause many
46 problems in the environment depending on the volume of the oil spilled. ^[2] For instance, water
47 resources as well as habitats where fish, birds, and other wildlife live can be damaged. ^[3] To address
48 this problem, oil wastewater treatment methods traditionally have included phase-separation and
49 skimming, evaporation, filtration and dissolved air flotation. However, these methods transform the
50 pollutants from one phase to another without mineralizing them. In other words, these methods are
51 non-destructive and generate lower volumes of more concentrated waste. Furthermore, these
52 methods are also less effective in removing the smaller oil droplets and emulsion. ^[4, 5]

53
54 Advanced oxidation processes (AOPs) have emerged as alternative wastewater treatment methods
55 which are environmentally friendly producing harmless end-products such as CO_2 and H_2O_2 . AOPs
56 are in-situ treatment processes characterized by the generation of highly reactive intermediates (OH
57 radicals) which can oxidise the target organic pollutants. ^[6] Photo-Fenton's reagent is one of the

58 AOPs that require iron ions in the presence of hydrogen peroxide and UV radiation to produce the
59 hydroxyl radicals. The Photo-Fenton reaction occurs in two steps:

60

61 (1) Fe^{2+} ions are oxidized by H_2O_2 producing OH radicals and Fe^{3+} ;

62 (2) Fe^{3+} is then reduced again to Fe^{2+} by the effect of UV light to produce more $\cdot\text{OH}$.^[7]

63

64 Photo-Fenton's reagent is one of the more widely applied AOPs since it is effective in treating
65 different kinds of wastewater. For instance, Rivas et al.^[8] investigated the treatment of the olive oil
66 mills wastewater by Fenton's reagent and the result was a positive influence on TOC (total organic
67 carbon). In addition, the treatment of the complex oily wastewater obtained from a lubricant
68 production using Fenton's reagent in the presence of the ultraviolet light was investigated by
69 Philippopoulos and Pouloupoulos.^[9] Moraes et al.^[10] applied the Photo-Fenton process in the
70 treatment of the wastewater contaminated with hydrocarbons using model raw gasoline oil. The
71 impact of hydrogen peroxide, iron and sodium chloride concentrations on process performance was
72 evaluated using the TOC technique; their results demonstrated that the Photo-Fenton process is a
73 feasible treatment process for this wastewater. Coelho et al.,^[11] concluded that a satisfactory
74 treatment by the Photo-Fenton treatment process was obtained in the case of a petroleum refinery
75 wastewater, achieving over 80% reduction in DOC (dissolved organic carbon). The treatment of the
76 contaminated wastewater with gasoline by the Photo-Fenton method was carried out by Galvao et
77 al.^[12], resulting in the TOC removal of 99% compared with 71% when the UV/ H_2O_2 process was
78 used.

79

80 The concentrations of the ferrous ions (Fe^{2+}), hydrogen peroxide (H_2O_2) and the pH of the
81 wastewater are the most important factors in determining the efficiency of the Photo-Fenton
82 treatment process. Optimization of these parameters is an obvious research goal. A statistical
83 technique known as the response surface methodology (RSM) was used to optimize these variables.

84 ^[13] RSM has previously been applied to optimize the Photo-Fenton treatment process in the
85 treatment of contaminated soil and wastewater. ^[14, 15, 16]

86 The study presented below describes the application of the Photo-Fenton reagent to the
87 mineralization of a synthetic diesel-oil wastewater emulsion and a 'real' car-wash wastewater
88 contaminated with diesel oil. The effect of the reaction operating conditions was investigated and
89 the RSM methodology was used to maximize COD removal rates.

90

91 **MATERIALS AND METHODS**

92 **Materials**

93 Commercial diesel oil was used as the model pollutant using sodium dodecyl sulphate ($C_{12}H_{25}Na_4S$)
94 emulsifier to prepare the oil-water emulsion. Car-wash wastewater collected at a petroleum filling
95 station was the source of the 'real' wastewater effluent. Ferrous chloride tetrahydrate ($FeCl_2 \cdot 4H_2O$)
96 and hydrogen peroxide (H_2O_2 ; 30 wt %) from Sigma-Aldrich were used as the source of the
97 Fenton's reagent. Sulphuric acid was used to adjust pH. For the radiated experiments a UV lamp
98 (high intensity 254nm UV, model R-52Grid Lamp) was used as a source of the UV light.

99

100 **Preparation of the Oil-water Emulsion**

101 Oxidation experiments were performed on the synthetic oil-water emulsion obtained by adding 2.5
102 mL of 0.1 g/L emulsifier solution to 1L of distilled water to which a 100 mL of diesel oil was added
103 gradually while stirring. The resulting emulsion was then stirred using a magnetic stirrer for 24
104 hours and left to stand for 1 hour to ensure separation of the non-dispersed oil in the water. The
105 supernatant was then filtered using a quantitative filter paper (Whatman 22 μm), generating an
106 emulsion with a COD (chemical oxygen demand) concentration of 1500 mg/L. This emulsion was
107 then diluted with distilled water to produce emulsion concentrations in the range of 200 to 800 mg-
108 COD/L.

109

110 **Car-wash Wastewater**

111 'Real' wastewater samples were collected from a car washing wastewater tank at a petroleum filling
112 station in the south of Dublin City, Ireland. The principal properties of this wastewater are: 82 mg-
113 COD/L, pH 8.2 and a suspended solids of 55 mg/L. To ensure saturation of the wastewater with
114 diesel oil, some samples, after the collection, were subjected to 24 hours of stirring following the
115 addition of the commercial diesel oil (100 mL/L). Thereafter, the wastewater, augmented with
116 diesel oil, was filtered through a quantitative filter paper (Whatman 22 μm) to produce an emulsion
117 with a COD of 404 mg-COD/L.

118

119 **Experimental Procedure**

120 The experiments were carried out in a batch mode at laboratory-scale using a 250 mL beaker.
121 Firstly, to produce the hydroxyl radicals, ferrous ions were added to a 200 mL sample of the
122 wastewater. The Fenton reaction was then enhanced by adding hydrogen peroxide. In the case of
123 the experiments where the effect of the pH was examined, the pH of the emulsion was adjusted by
124 adding sulphuric acid before Fenton's reagent was added. Thereafter, the mixture was subjected to
125 magnetic stirring and UV radiation (254nm wavelength), as illustrated in Fig. 1. Samples were
126 taken at a regular time intervals to determine the degree of COD removal from the wastewater. In
127 order to investigate different AOPs, experiments were conducted using UV-photolysis alone
128 Fenton's reagent without UV radiation and compared with the Fenton's reagent with the UV
129 radiation (Photo-Fenton). In addition, the effect of the initial concentration of oil-water emulsion,
130 the pH and the initial concentration of H_2O_2 and Fe^{2+} were studied.

131

132 **Analytical Methods**

133 Measurements of COD were performed using the HACH instrument (model HACH DR-2400) in
134 order to measure the effect of AOPs on the mineralization of the emulsion and for each

135 measurement, three samples were taken and the average value is reported. The pH of the emulsion
136 was measured using a digital pH-meter (model PHM62 supplied by Mason).

137

138 **RESULTS AND DISCUSSION**

139 **Comparison of Different Degradation Systems**

140 Fig. 2 shows the investigation of the different AOPs and the comparison of their performance with
141 the Photo-Fenton's reagent. The doses for the Fenton's reagent were: $[\text{Fe}^{2+}] = 40 \text{ mg/L}$; $[\text{H}_2\text{O}_2]$
142 $=100 \text{ mg/L}$ and the starting pH of the emulsion was 8 without any adjustment. Examination of the
143 results shows that the UV-photolysis without the Fenton's reagent addition only achieved a 5%
144 reduction after 6 hours in the COD concentration. However, Fenton's reagent alone achieved a
145 COD reduction of 42%. Clearly, the reaction between the ferrous ions and hydrogen peroxide
146 produced the $\cdot\text{OH}$ radicals which played an important role in the oil degradation. As reported in the
147 literature, ^[17] diesel oil consists of aromatic compounds and Fenton's reagent is efficient in the
148 destruction of these aromatic compounds. The $\cdot\text{OH}$ radicals attack these aromatic compounds
149 opening the rings and producing reaction intermediates which are ultimately converted to harmless
150 end products such as CO_2 and H_2O . Furthermore, when the UV was used in conjunction with the
151 Fenton's reagent in the Photo-Fenton process a more pronounced degradation was obtained (COD
152 reduction=50%). The UV photolysis in addition the chemical reagent enhanced the generation of
153 more reaction hydroxyl intermediates which resulted in enhanced degradation of the pollutants.
154 These observations are in accordance with that obtained by Moraes et al. ^[17] and Galvao et al. ^[12]

155

156 **Effect of the Initial Emulsion Concentration**

157 The effect of the initial concentration of the oil-water emulsion on its photo-catalytic degradation is
158 shown in Fig. 3. It is clear from Fig. 3 that the reaction rate is increased by decreasing the initial
159 emulsion concentration and the percentage COD removals are 60, 71, 72, 75, 82 for the initial
160 emulsion concentrations of 1500, 800, 600, 400 and 200 mg-COD/L, respectively. The increasing

161 percentage COD removal with decreasing initial COD concentration can be attributed to the
162 decrease in turbidity of the emulsion. The emulsion turbidity for an initial COD of 1500 mg/L was
163 49 NTU, whereas when the initial COD was 200 mg/L the emulsion turbidity was only 5 NTU.
164 Decreasing turbidity clearly enhances the penetration of the UV light, resulting in enhanced COD
165 removal. This observation of increasing the photo-catalytic reaction rate with decreasing the initial
166 pollutant concentration was also reported by Najjar et al., ^[19] in the photo-catalytic degradation of
167 the nitrophenol.

168

169 **Effect of Iron Concentration**

170 Photo-Fenton treatment of the emulsion was undertaken at different Fe^{2+} concentrations (10-100
171 mg/L) to examine the role of Fe^{2+} concentration in the Photo-Fenton degradation process. The
172 results in Fig. 4 show that the mineralization rate increased with Fe^{2+} concentration, the optimal
173 value being 40mg/L which results in a 60% removal of COD after 150 minutes of reaction time.
174 Iron concentrations above this optimal value result in reduced process performance because more
175 species of iron ions are produced rather than the more useful $\cdot\text{OH}$ radicals. This finding is in
176 agreement with the previous observation of Kositzki et al. ^[20]

177

178 **Effect of H_2O_2 Concentration**

179 To investigate the effect of hydrogen peroxide on the Photo-Fenton treatment process the
180 concentration of the former was varied and all the other parameters were kept constant. The results,
181 illustrated in Fig. 5, show a significant enhancement of the degradation process when the H_2O_2
182 concentration was increased from 50 mg/L to 400 mg/L. Increasing H_2O_2 concentration results in
183 the generation of additional reaction intermediates ($\cdot\text{OH}$) radicals which enhances the degradation
184 process. However, at higher peroxide concentrations, the excess hydrogen peroxide can act as an
185 $\cdot\text{OH}$ scavenger, forming $\text{HO}_2\cdot$, which is also a free radical produced in-situ from the H_2O_2 but is a

186 less reactive oxidizing agent and therefore has a longer life time than the $\cdot\text{OH}$ and the result is a
187 reduction in the overall reaction rate. [21-23]

188

189 **Effect of the Initial pH**

190 As the effect of the pH plays an important role in the Photo-Fenton treatment process, its
191 dependence was studied by varying the initial pH of the emulsion. [12, 20, 24, 25] The natural pH of the
192 oil-water emulsion was 8.5. In this study, pH in the range 2 to 8.5 was examined. The natural pH of
193 the wastewater was altered by adding sulphuric acid. It is clear from the results in Fig. 6 that the
194 performance of the Photo-Fenton process is highly dependent on the initial pH of the aqueous
195 emulsion. The optimal performance was found to be at the pH of the emulsion without any
196 adjustment. These results imply that the initial pH plays an important role in the initiation of the
197 reaction intermediates. In other words, pH is the controlling parameter in the hydrogen peroxide
198 decomposition; at very low pH, the peroxide decomposes slowly and the reaction rate becomes very
199 slow. [24]

200 The optimal pH value found in this case accords with the findings of Philippopoulos and
201 Pouloupoulos [9] who found that an alkaline pH was most effective in the Fenton treatment process of
202 wastewater polluted with phenol solution. However, Paterlini and Nogueira [7] found that an acidic
203 pH (2.5) was best for the treatment of an herbicide solution. Moreover, Kang and Hwang also found
204 the pH in the range 2.5-4 to be the most efficient pH for the treatment by Fenton's reagent of the
205 landfill leachate. [25] Thus, it is reasonable to conclude that the optimum pH for Photo-Fenton
206 wastewater treatment is very dependent on the wastewater composition.

207

208 **Application of Photo-Fenton's Reagent to 'Real' Wastewater**

209 The applicability of this technology to the treatment of 'real' wastewater is demonstrated in the case
210 of car-wash wastewater sourced at a petroleum filling station. The optimum concentrations of
211 Fenton's reagent determined in the experiments using the synthetic oil-water emulsion were applied

212 to the 'real' car-wash wastewater: $Fe^{2+}] = 40 \text{ mg/L}$; $[H_2O_2] = 400 \text{ mg/L}$. The pH of the wastewater
213 was 8.2 and no adjustment was made. The wastewater was continuously stirred in the presence of
214 the UV light for a total reaction time of 4 hours. The results of this experiment are graphically
215 illustrated in Fig. 7 and demonstrate the ability of the Photo-Fenton method to degrade this
216 wastewater. A second experiment was under taken with this 'real' wastewater augmented with
217 diesel oil. Examination of Fig. 7 shows that, although the initial COD concentrations of 'real'
218 wastewater (82 mg/L) and the 'real' wastewater augmented with diesel oil (404 mg/L) significantly
219 differ, the rates of degradation are similar in both cases. It should also be noted that the 'model' and
220 'real' wastewater rates of degradation are also comparable.

221

222

223 **STATISTICAL ANALYSIS OF PHOTO-FENTON PROCESS**

224 Optimization of the Photo-Fenton treatment process (by determining the optimum of the
225 independent variables; Fe^{2+} , H_2O_2 and pH) to degrade the oil-water emulsion was conducted using
226 the response surface methodology (RSM) design. ^[13] As indicated in Table 1, fifteen sets of
227 experimental data were used in the numerical analysis. A Box-Behnken factorial design and
228 analysis of the experimental data was undertaken. ^[13] In the numerical analysis (see Table 1) the
229 Fe^{2+} concentration, H_2O_2 concentration and initial pH are denoted as X_1 , X_2 and X_3 , respectively,
230 corresponding to their experimental values x_1 , x_2 and x_3 . The experimental data collected was
231 analysed by performing the analysis of variance (ANOVA) using the Statistical Analysis System
232 (SAS) ^[26] and fitted with a second-order polynomial model. The following response function (1)
233 was used to correlate the dependent and independent variables in the response surface:

$$234 \quad S = \beta_0 + \sum \beta_i X_i + \sum \beta_{ii} X_i^2 + \sum \sum \beta_{ij} X_i X_j \quad (1)$$

235 where S is the predicted response (COD removal, %); the model regression coefficients are: β_0 the
236 constant coefficient, β_i the linear coefficients, β_{ii} the quadratic coefficients and β_{ij} are the model
237 regression coefficients; X_i and X_j are the independent variables. Mathematica software version 5.2.

238 was used to obtain the optimum conditions for the operating variables and for the COD percentage
 239 removal. The response surfaces of two-dimensional contour plots and three-dimensional curves
 240 were developed using MATLAB 7 software. The experiments were planned and conducted
 241 according to the three-level factorial Box-Behnken design ^[13] as presented in Table 2. Analysis of
 242 the data by SAS yielded the following second order polynomial equation:

243

$$244 \quad S(\%) = 63.797 - 2.94X_1 - 0.324X_2 + 5.60X_3 - 9.56X_1^2 + 2.08X_1X_2 - 4.12X_1X_3 \quad (2)$$

$$245 \quad -16.66X_2^2 + 0.58X_2X_3 - 0.55X_3^2$$

245

246 Table 2 presents a statistical analysis of the data by SAS. The analysis was done by means of the
 247 coefficient of correlation (R^2) of the experimental data and by means of Fisher's (F) test. The
 248 correlation coefficient is a measure of the goodness of fit between the model and experimental data.
 249 The F test is used to determine the significance of the regression coefficients of the parameters. The
 250 analysis of variance table is composed of the following columns: Source (the source of the
 251 variation); DF (the degree of freedom); SS (the sums of squares); MS (the mean squares); Fisher F
 252 values; Probability P values. The sum of the squares (SS) is the summation of the squares of the
 253 dependent variables. The mean squares (MS) column lists the mean squares which are the sums of
 254 squares divided by the degree of freedom. The F value is defined as follows:

255

$$256 \quad F \text{ value} = \frac{\text{Between groups variance}}{\text{Pooled variance}} \quad (3)$$

257

258 In general, the larger the magnitude of the F and the smaller the value of P (the probability of
 259 exceedance of F) the more significant is the corresponding coefficient term. The model is
 260 significant when the P -value is less than 0.05. ^[13, 26, 27] Examination of the table shows that the
 261 model is highly significant as the Fisher F -test is 8.476 with a low probability (P) of exceedance
 262 value of 0.0149. The high correlation coefficient (R^2) of 0.94 demonstrates how well the model fits

263 the experimental data (as shown in Fig. 8), the model being rejected if the R^2 value is less than 0.8.
264 ^[13, 26] By fixing one parameter at its zero level, it was possible to graphically represent the
265 relationship between the percentage COD removal and the other two independent variables using
266 MATLAB 7.0 (Figs. 9-11). The optimum values of the selected variables in the Photo-Fenton
267 process were obtained using Mathematica software (V 5.2): $[\text{Fe}^{2+}] = 33 \text{ mg/L}$; $[\text{H}_2\text{O}_2] = 397 \text{ mg/L}$;
268 $\text{pH} = 8.5$; COD percentage removal = 70.

269

270 Table 3 provides the comparison of the results obtained in the literature with those from the
271 presented study. With the exception of ^[29], removal efficiencies reported in the literature for
272 gasoline/diesel wastewaters varied from 66% to 96%, the present study being 70%. The range of the
273 removal efficiencies is attributable to the variety of hydrocarbon compounds and their
274 concentrations in the wastewaters.

275

276 CONCLUSIONS

277 The present study demonstrates the suitability of advanced oxidation processes for the treatment of
278 oil-water emulsion and car-wash wastewater. The Photo-Fenton process using the artificial UV light
279 is more efficient than the Fenton and UV-radiation treatment processes on their own. After 150 min
280 of the Photo-Fenton reaction, the COD removal rate ranged from 60-82 %, depending on the initial
281 concentration of the emulsion (for the concentration range 1500-200 mg-COD/L, respectively).
282 However, after 240 minutes reaction time, the final COD percentage removals achieved were 74%
283 for the car-wash wastewater and 65% for the car-wash wastewater augmented with the diesel oil.
284 Moreover, the removal efficiencies were improved by increasing the hydrogen peroxide and ferrous
285 ion concentrations, but once $[\text{Fe}^{2+}]_0$ and $[\text{H}_2\text{O}_2]_0$ concentrations exceeded 40 and 400 mg/L
286 respectively little improvement resulted. Finally, an increase in the efficiency of the COD removal
287 from this wastewater could be achieved by optimizing the Photo-Fenton parameters using RSM.
288 The maximum response (COD percentage removal) exceeded 70 % for the initial emulsion

289 concentration of 800 mg-COD/L using the optimum values of 33 and 397 mg/L for Fe²⁺ and H₂O₂,
290 respectively at a pH of 8.5.

291

292

293

294 **ACKNOWLEDGMENTS**

295 Maha Tony gratefully thanks the Ministry of Higher Education, Missions Department, Egypt for the
296 financial support granted through the Channel Scheme Mission. The authors would like to thank
297 Mr. P. Kearney for his technical assistance during this study.

298

299

300 **REFERENCES**

- 301 1. <http://www.waterqualityresearch.com/Documents/MTBE.pdf>
- 302 2. Biswas, S.; Chaudhari, S. K., Mukherj, S. Microbial uptake of diesel oil sorbed on soil and oil
303 spill clean-up sorbents. *J. Chem. Technol. Biotechnol.* **2005**, *80*, 587–593.
- 304 3. Kim, I. Ten years after the enactment of the Oil Pollution Act of 1990: a success or a failure.
305 *Mar. Policy*, **2002**, *26*, 197–207.
- 306 4. Portela, J.R.; Sanchez-Oneto, J.; Lopez, J.; Nebot, E.; Ossa, E.M. Hydrothermal oxidation of oily
307 wastes: An alternative to conventional treatment methods. *Eng. Life Sci.* **2003**, *3* (2), 85-89.
- 308 5. Li, Y.S.; Yan, L.; Xiang, C.B.; Hong, L.J. Treatment of oily wastewater by organic–inorganic
309 composite tubular ultrafiltration (UF) membranes. *Desalination.* **2006**, *196*, 76–83.
- 310 6. Seo, D.C.; Lee, H.J.; Hwang, H.N.; Park, M.R.; Kwak, N.W.; Cho, I.J.; Cho, J.S.; Seo, J.Y.; Joo,
311 W.H.; Park K.H.; Heo, J.S. Treatment of non-biodegradable cutting oil wastewater by
312 ultrasonication-Fenton oxidation process. *Water Sc. Technol.* **2007**, *55* (1–2), 251–259.
- 313 7. Paterlini, W.C.; Nogueira, R.F.P. Multivariate analysis of Photo-Fenton degradation of the
314 herbicides tebuthiuron, diuron and 2,4-D. *Chemosphere.* **2005**, *58*, 1107–1116.

- 315 8. Rivas, F.J.; Beltran, F.J.; Gimeno, O.; Frades, J. Treatment of olive oil mill wastewater by
316 Fenton's reagent. *J. Agric. Food Chem.* **2001**, *49*, 1873-1880.
- 317 9. Philippopoulos, C.J.; Pouloupoulos, S.G. Photo-assisted oxidation of an oily wastewater using
318 hydrogen peroxide. *J. Hazard. Mater.* **2003**, *B98*, 201–210.
- 319 10. Moraes, J.E.F.; Quina, F.H.; Nascimento, C.A.O.; Silva, D.N.; Filho, O.C. Treatment of Saline
320 Wastewater contaminated with hydrocarbons by the Photo-Fenton process. *Environ. Sci.*
321 *Technol.* **2004**, *38*, 1183-1187.
- 322 11. Coelho, A.; Castro, A.V.; Dezotti, M.; Sant'Anna, G.L. Treatment of petroleum refinery
323 sourwater by advanced oxidation processes. *J. Hazard. Mater.* **2006**, *B137*, 178–184.
- 324 12. Galvao, S.A.O.; Mota, A.L.N.; Silva, D.N.; Moraes, J.E.F.; Nascimento, C.A.O.; Chiavone-
325 Filho, O. Application of the Photo-Fenton process to the treatment of wastewaters contaminated
326 with diesel. *Sci. Total Environ.* **2006**, *367*, 42–49.
- 327 13. Montgomery, D.C. *Design and Analysis of Experiments*. John Wiley, New York, 1991.
- 328 14. Watts, R.J.; Stanton, P.C.; Howsawkung, J.; Teel, A.L. Mineralization of a sorbed polycyclic
329 aromatic hydrocarbon in two soils using catalyzed hydrogen peroxide. *Water Res.* **2002**, *36*
330 (17), 4283–4292.
- 331 15. Torrades, F.; Perez, M.; Mansilla, H.D.; Peral, J. Experimental design of Fenton and Photo-
332 Fenton reactions for the treatment of cellulose bleaching effluents. *Chemosphere.* **2003**, *53*,
333 1211-1220.
- 334 16. Teel, A.L.; Warberg, C.R.; Atkinson, D.A.; Watts, R.J. Comparison of mineral and soluble iron
335 Fenton's catalyts for the treatment of trichloroethylene. *Water Res.* **2001**, *35* (4), 977–984.
- 336 17. Frusteri, F.; Spadaro, L.; Beatrice, C.; Guido C. Oxygenated additives production for diesel
337 engine emission improvement, *Chem. Eng. J.* **2007**, *134*, 239–245.
- 338 18. Moraes, J.E.F.; Silva, D.N.; Quina, F.H.; Chiavone-Filho, O.; Nascimento, C.A.O. Utilization of
339 Solar Energy in the Photodegradation of Gasoline in Water and of Oil-Field-Produced Water.
340 *Environ. Sci. Technol.* **2004**, *38*, 3746-3751.

- 341 19. Najjar, W.; Chirchi, L.; Santosb, E.; Ghorhel, A. Kinetic study of 2-nitrophenol
342 photodegradation on Al-pillared montmorillonite doped with copper. *J. Environ. Monit.* **2001**, *3*,
343 697–701.
- 344 20. Kositzki, M.; Poulios, I.; Malato, S.; Caceres, J.; Campos, A. Solar photocatalytic treatment of
345 synthetic municipal wastewater. *Water Res.* **2004**, *38*, 1147-1154.
- 346 21. Chu, W. Modeling the quantum yields of herbicide 2, 4-D decay in UV/H₂O₂ process.
347 *Chemosphere.* **2001**, *44*, 935–941.
- 348 22. Litorja, M.; Ruscic, B. A photoionization study of the hydroperoxyl radical, HO₂, and hydrogen
349 peroxide, H₂O₂, *Journal of Electron Spectroscopy and Related Phenomena*, **1998**, *97*, 131–146.
- 350 23. Cember, H. *Introduction to health physics.* Mc Graw-Hill, 1996, 237.
- 351 24. Kim S.M.; Vogelpohl, A. Degradation of Organic Pollutants by the Photo-Fenton-Process.
352 *Chem. Eng. Technol.* **1998**, *21* (2), 187-191.
- 353 25. Kang, Y.W.; Hwang, K. Effect of reaction conditions on the oxidation efficiency in the process.
354 *Water Res.* **2000**, *34* (10), 2786-2790.
- 355 26. SAS, *SAS /STAT User's Guide.* SAS Institute, Inc., Cary, NC, 1990.
- 356 27. Meard, R. *The design of experiments: statistical principles for practical application.* Cambridge
357 university press, 1988.
- 358 28. Gernjak, W.; Maldonado, M.I.; Malato, S.; Caceres, J.; Krutzler, T.; Glaser, A.; Bauer, R. Pilot-
359 plant treatment of olive mill wastewater (OMW) by solar TiO₂ photocatalysis and solar Photo-
360 Fenton. *Sol. Energy.* **2004**, *77*, 567–572.
- 361 29. Tiburtius, E.R.L.; Peralta-Zamora, P.; Emmel, A. Treatment of gasoline-contaminated waters by
362 advanced oxidation processes. *J.Hazard. Mater.* **2005**, *B126*, 86–90.
- 363
- 364
- 365
- 366

367

368

369 **LIST OF TABLES:**

370

371

Table 1. Statistical Analysis System (SAS) input and output data

Experiment number	Measured concentrations			Codified values*			Response (<i>COD removal</i>)	
	Fe ²⁺ (mg/L)	H ₂ O ₂ (mg/L)	pH	X ₁ Fe ²⁺	X ₂ H ₂ O ₂	X ₃ pH	Experimental	Predicted
1	20	200	6	-1	-1	0	39.30	42.92
2	20	600	6	-1	1	0	38.00	38.12
3	60	200	6	1	-1	0	33.00	32.88
4	60	600	6	1	1	0	40.00	36.38
5	40	200	3.5	0	-1	-1	46.30	41.88
6	40	200	8.5	0	-1	1	51.00	51.93
7	40	600	3.5	0	1	-1	41.00	40.08
8	40	600	8.5	0	1	1	48.01	52.44
9	20	400	3.5	-1	0	-1	46.11	46.92
10	60	400	3.5	1	0	-1	44.71	49.26
11	20	400	8.5	-1	0	1	70.90	66.35
12	60	400	8.5	1	0	1	53.02	52.22
13	40	400	6	0	0	0	63.57	63.80
14	40	400	6	0	0	0	63.12	63.80
15	40	400	6	0	0	0	64.70	63.80

$$* X_i = \frac{(x_i) - (\text{its upper level} + \text{its lower level})/2}{(\text{its upper level} - \text{its lower level})/2}$$

372

373

374

Table 2. Analysis of Variance (ANOVA) for response surface

Source	Degree of freedom (df)	Sum of squares (SS)	Mean squares (MS)	Fisher <i>F</i> -value	<i>Probability</i> <i>P</i> -value
Model	9	1694.01	188.2234	8.476099	0.014948
Linear	3	321.3326	321.3326	14.47029	1.01074
Square	3	1363.768	1363.768	61.41336	0.84254
Interaction	3	86.45413	86.45413	3.893213	1.375712
Error	5	111.0318	22.20637		
Total	14	1805.042			

$$R^2 = 93.85 \% ; \text{adj } R^2 = 82.78 \%$$

375

376

377

378

379
380

Table 3. Comparison of results from literature with those from present study

Type of wastewater	Initial organic concentration	Experimental conditions				UV source	% organic removal	Ref.
		[Fe ⁺⁺], mg/L	[H ₂ O ₂], mg/L	pH	Reaction time (h)			
Synthetic emulsion of diesel wastewater	800 mg-COD/L	33 mg/L (FeCl ₂ ·4H ₂ O)	397 (30%, m/v)	8.5	2	254nm high intensity UV lamp	70% (COD removal)	This study
Synthetic gasoline wastewater	80-90 mg-TOC/L	(FeSO ₄ ·7H ₂ O) 1mM	3400 (30%)	3	4.5	450W medium pressure Hg UV lamp	96% (TOC removal)	[10]
Sourwater from petroleum refinery	850-1020 mg-COD/L	(FeSO ₄) 1100 mg/L	15400 (30%)	8	1	250 W Hg vapor UV lamp	83% (DOC removal)	[11]
Synthetic emulsion of diesel wastewater	-	(FeSO ₄ ·7H ₂ O) 0.1 mM	170 (30%)	3	0.5	450 W medium pressure UV lamp	67% (TOC removal)	[12]
Synthetic emulsion of gasoline wastewater	70-80 mg-TOC/L	(FeSO ₄ ·7H ₂ O) 1 mM	3400 (30%)	3	3	450W Hg UV lamp	66-91% (TOC removal)	[18]
Olive mill wastewater	34000 mg-COD/L	(FeSO ₄) 5 mM	5000 (30%)	2.8	12	Solar UV source	50% (COD removal)	[28]
Synthetic gasoline wastewater	-	(FeSO ₄ ·7H ₂ O) 10 mg/L	500 (10%)	3	1.5	125 W medium pressure Hg UV lamp	20% (Evaluated by fluorescence spectroscopy)	[29]

FIGURE CAPTIONS:

Figure 1. Schematic diagram of the experimental set-up

Figure 2. Effect of different degradation systems on the oil-water emulsion (Fenton and Photo-Fenton reagents: $[\text{Fe}^{2+}] = 40 \text{ mg/L}$; $[\text{H}_2\text{O}_2] = 100 \text{ mg/L}$, $\text{pH} = 8$)

Figure 3. Effect of the initial emulsion concentration (operating parameters: $[\text{Fe}^{2+}] = 40 \text{ mg/L}$; $[\text{H}_2\text{O}_2] = 400 \text{ mg/L}$; $\text{pH} = 8$)

Figure 4. Effect of the iron concentration on the Photo-Fenton treatment process (operating parameters: $[\text{H}_2\text{O}_2] = 400 \text{ mg/L}$; $\text{pH} = 8$)

Figure 5. Effect of the H_2O_2 concentration on the Photo-Fenton treatment process (operating parameters: $[\text{Fe}^{2+}] = 40 \text{ mg/L}$; $\text{pH} = 8$)

Figure 6. Effect of pH on the Photo-Fenton treatment process (operating parameters: $[\text{Fe}^{2+}] = 40 \text{ mg/L}$; $[\text{H}_2\text{O}_2] = 400 \text{ mg/L}$)

Figure 7. Effect of the Photo-Fenton's reagent on the car-wash wastewater ($[\text{Fe}^{2+}] = 40 \text{ mg/L}$; $[\text{H}_2\text{O}_2] = 400 \text{ mg/L}$; $\text{pH} = 8.2$)

Figure 8. Plot of the measured COD removal (%) against the predicted values from the second order response surface model, ($R^2 = 0.94$)

Figure 9. 3-D surface and contour plot of the predicted % COD removal (S, %) showing the effect of the X_1 (Fe^{2+} dose) and X_2 (H_2O_2 dose)

Figure 10. 3-D surface and contour plot of the predicted % COD removal (S, %) showing the effect of the X_1 (Fe^{2+} dose) and X_3 (pH)

Figure 11. 3-D surface and contour plot of the predicted % COD removal (S, %) showing the effect of the X_2 (H_2O_2 dose) and X_3 (pH)

LIST OF FIGURES:

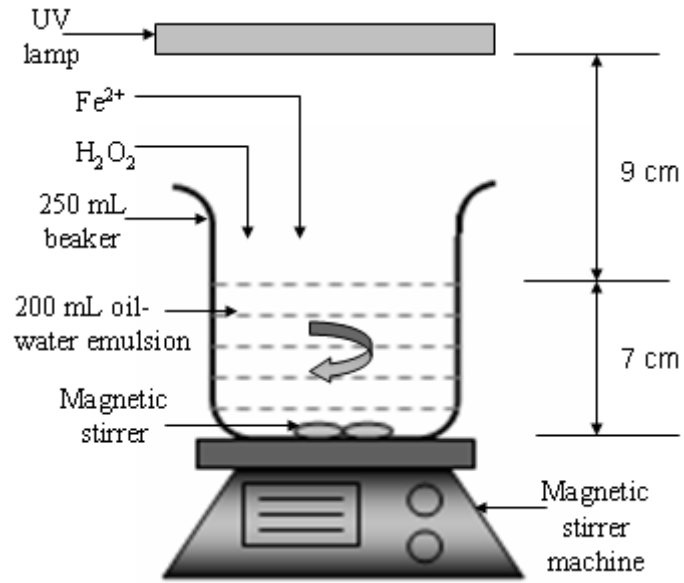


Fig. 1

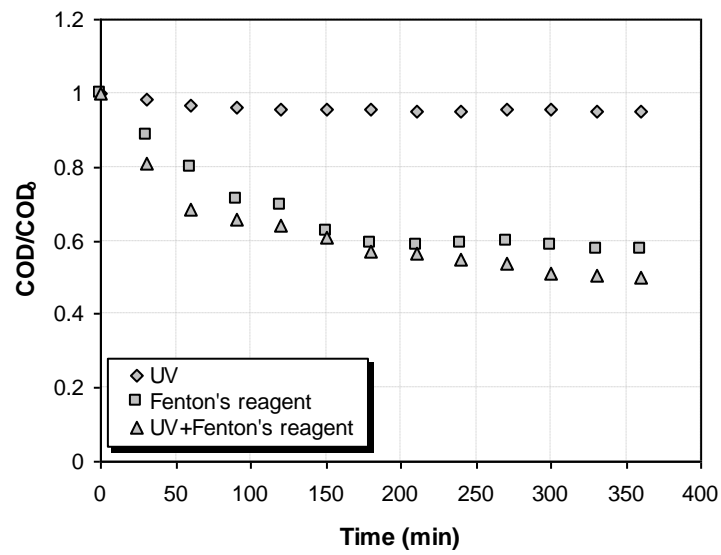


Fig. 2

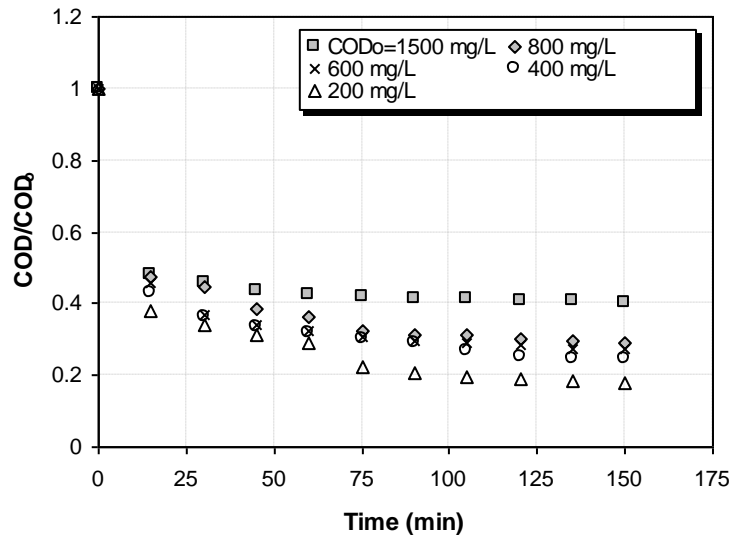


Fig. 3

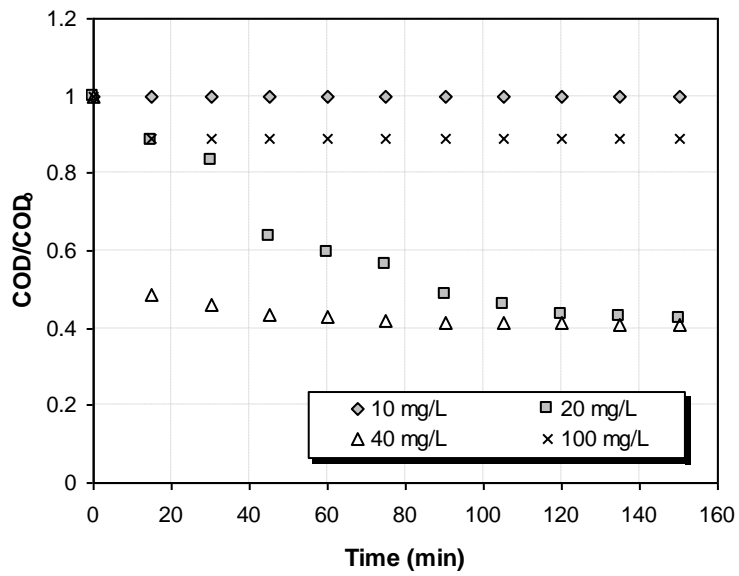


Fig. 4

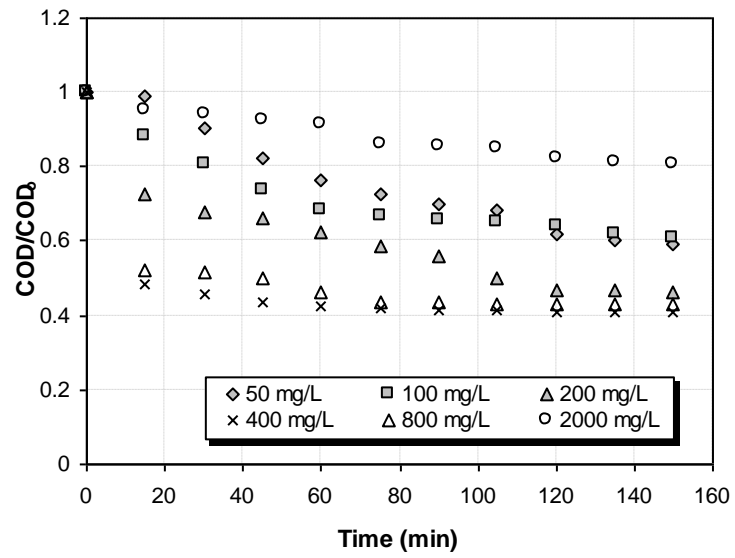


Fig. 5

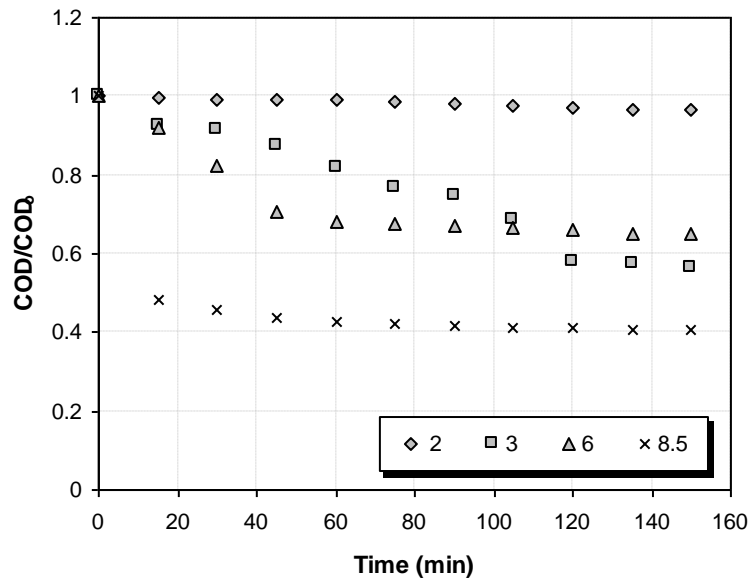


Fig. 6

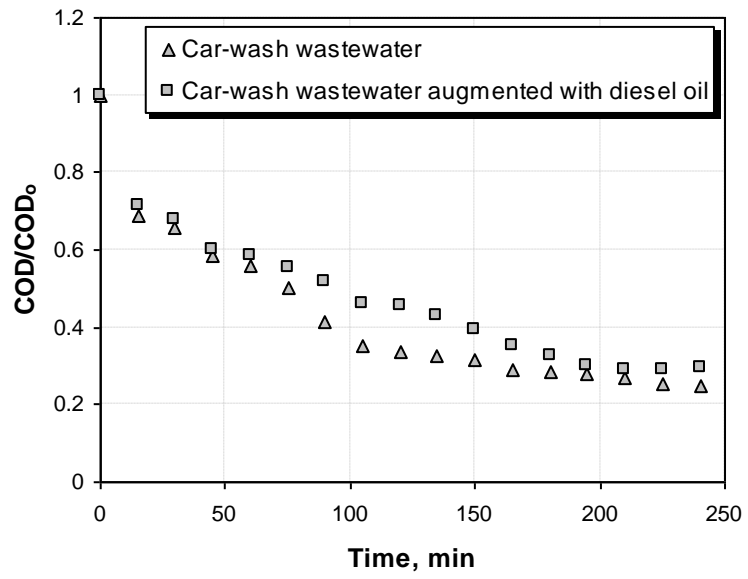


Fig. 7

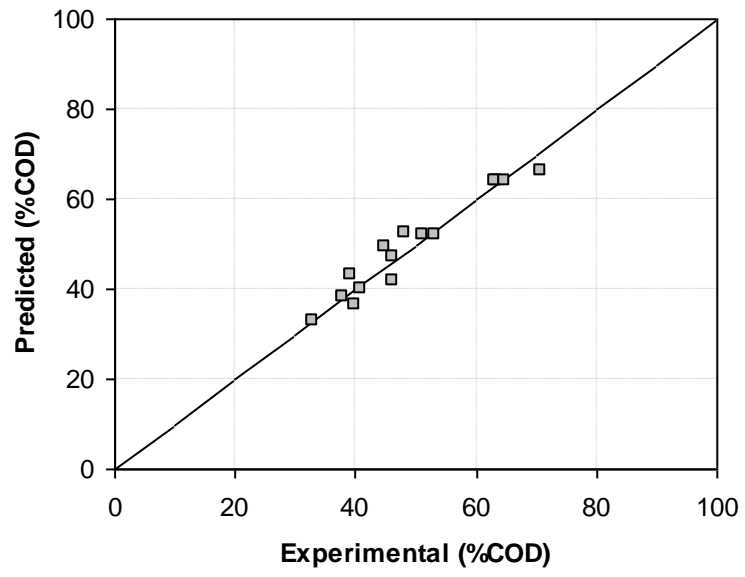


Fig. 8

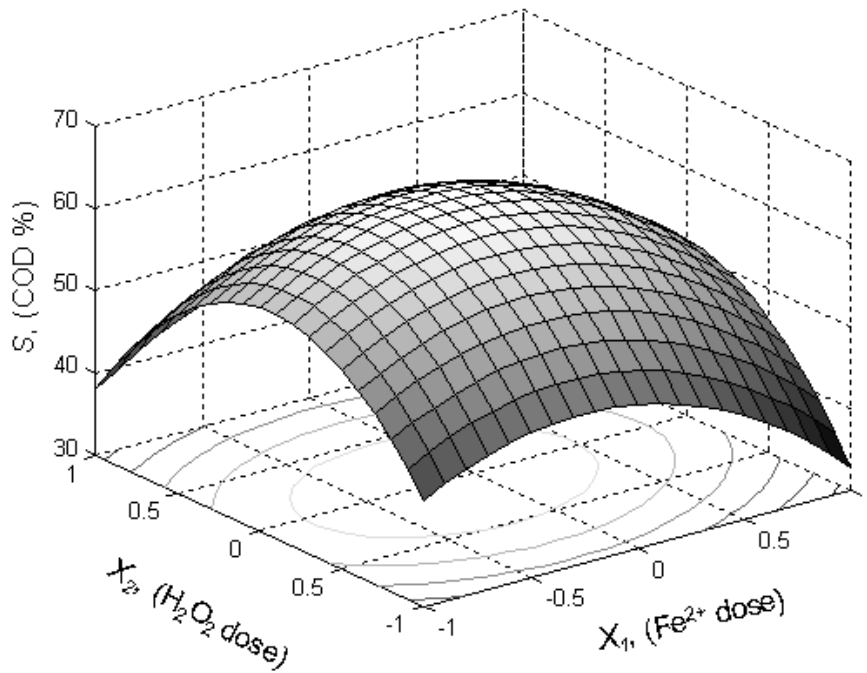


Fig. 9

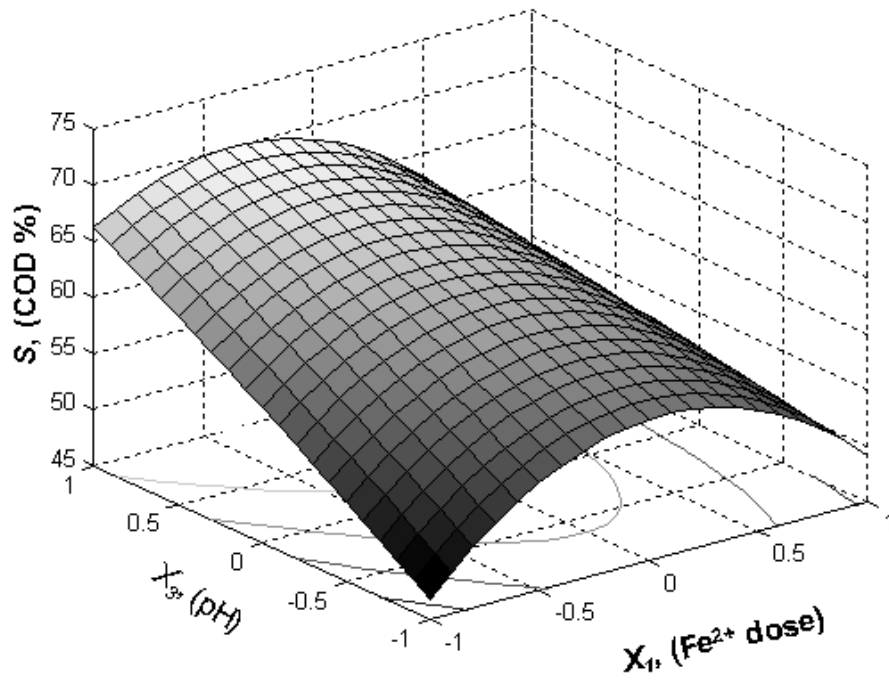


Fig. 10

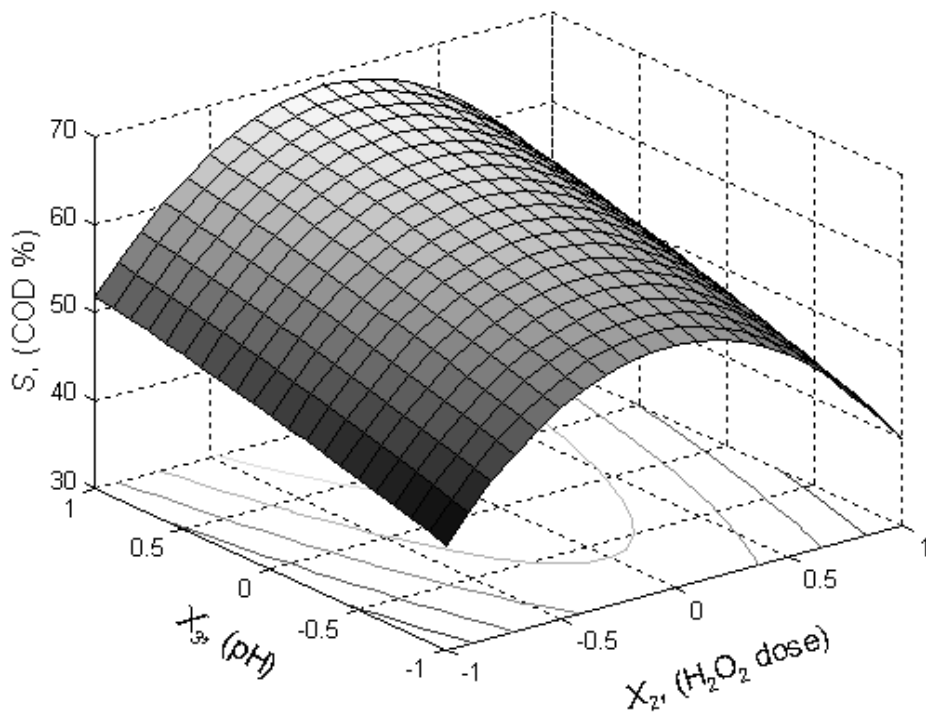


Fig. 11